Analysis of Surface Degradation of Silicon Rubber Insulators after 30 Years in-Service

Lunnetta Safura Lumba and Suwarno

School of Electrical Engineering and Informatics
Institut Teknologi Bandung
Bandung, Indonesia
lunnettasafura@gmail.com suwarno@stei.itb.ac.id

Abstract: In recent years, polymeric insulators have been increasingly used for high voltage overhead transmission lines. The industry has replaced the insulators from ceramic to polymeric due to its lightweight and hydrophobic materials, not to mention the performance against pollutant contamination. In this study, an analysis of two 70 kV silicone rubber insulators is performed. The insulators had been in service for 30 years on transmission networks in volcanic area, exposed to intense UV solar radiation in midday, but also high precipitation occur throughout the year. The urge to understand better of polymeric aging behavior is important to improve the quality of the polymeric type insulators. In this study, these aged samples were then compared with virgin samples to identify the endurance and quality of polymer material. The surface deterioration and the change of chemical content were evaluated using advanced techniques, including Spectroscopy and Scanning Electron Microscopy (SEM), Energy-dispersive X-ray Analysis (EDX), Thermo-Gravimetric Analysis (TGA), and Fourier Transform Infrared (FTIR). Meanwhile, the hydrophobic and visual inspection were also conducted. The hydrophobicity was evaluated by measuring the contact angle and assessed using IEC62073. The aged samples are categorized as hydrophobic class 1 due to the angle value of more than 60°. Physicochemical results showed that the aged sample compared with the virgin simple did not differ significantly given that the aged samples have been in-service for 30 years. Based on TG/DTA result, the percentage difference of weight loss between virgin and aged sample only lower than 4%. Then, from EDX result, the atomic percentage differences of C and O component compared with virgin sample are 4%-10%. Furthermore, the FTIR spectra indicates a normal aging condition of the silicone rubber, the difference in peak value of $Si\text{-}(CH_3)_2$ and OH compared with virgin sample is 10%.

Keywords: Polymeric Insulator, Natural Aging, TGA, SEM/EDX, Leakage Current, FTIR

1. Introduction

Polymer has been widely used in many life aspects of modern life due to its versatile function, starting from daily life until the industrial scale of utilization. Most people minimally have contact with one polymer product, from drinking bottles to gadgets. In the industry and public sector, specifically in the electrical power field, the polymer has been used for a long time as insulating materials. One of the polymer products in the electrical power field is a polymeric insulator.

The insulator housing is commonly ethylene propylene diene monomer (EPDM), elastomer (one of type in silicone), or copolymers of silicone and EPDM [1]. Silicone rubber is a man-made polymer which characteristics are different from the natural-made rubber. It is a type of synthetic polymer with its backbone does not contain carbon or is called an inorganic polymer. The structure of silicone-oxygen bonds is highly stable [2]. This structure makes it possible to have high thermal resistance and electrical

The polymeric insulator is proven that is better than other types of insulators, for instance, glass insulator and ceramic insulator. The silicone sidechains deliver the polymer hydrophobic, resulted in fulfill the need to repel water, mostly in high polluted regions. Then, the other

Received: September 5th, 2020. Accepted: November 25th, 2020
DOI: 10.15676/ijeei.2020.12.4.8

benefit of the polymeric insulator, compared with the density of glass and ceramic insulator, this type is very light in weight with significant degrees of strength. Due to its performance, polymeric insulator does not require frequent maintenance and has a long lifetime.

Nevertheless, the limitations of a polymeric insulator due to several major issues still exist, which is the failure of a polymeric insulator due to the aging process. Weathering is believed as the main reason for aging and reduced life expectancy. This indeed leads to failure, but in truth are moisture and contaminant from the polluted environment [3-5]. Hydrophobicity gradually lost because of a continuous path of water droplets and a significant accumulation of the pollutant layer. This is the initial cause that led to dry band arching and insulator failure as the worst case.

Many researchers have studied polymeric insulator to understand the character and to improve the quality, which lead to the extension of its lifetime—ranging from testing modified filler of the housing to the characterization of existing material. Most of the research regarding polymeric insulator, they emphasize in the modification of sample testing and observe filler component material. It is essential to understand the field-aging process in specific environment. But mostly, the samples used for the study are the result of the artificial aging process. Because waiting for the samples aged as desire takes a long time, the artificial aging method is preferable. Hence, only a few studies are using natural-aging polymeric insulators as a sample.

In the previous research, the natural aged polymeric insulators were treated in a different environment and tested in various aspects, from material characterization to electrical testing. The study with a two-year in-service sample from the industrial area in Hattar City, Pakistan, conduct by Amin S. et al. showed a light degradation [7]. Sundarajan et al. analyzed the material degradation of 345 kV EPDM insulators after five years in service in the New Hampshire coastal area. They used advanced surface structural analysis and reported significant differences in surface properties between the chalked discolored and dark surface [8]. Meanwhile, the research which used the same aging duration, five years, showed different results. Fernando et al., whose used sample, whether from marine or heavily polluted environment, reported there was no severe damage [9]. Rowland et al. studied a sample from the coastal area in the UK, which had been operated for 15 years, and there was no significant reduced performance indicated [10]. Last, Mavrikakis et al. evaluated the oldest sample among all research before, 150 kV composite suspension insulators, which had been operated for 17 years in Greece's coastal area. Here the focus was that EPDM surface degradation was more intense than VMQ/HCR [11]. From the previously stated, most researchers used samples from the coastal area; it is rare to found other regions such as mountain areas or areas with high precipitation.

Indonesia, as an archipelagic state, has diverse regional functions and geographical features. Each region faces different problems correlated with the insulators. The capitals encounter with the heavily polluted industrial area, while the others are in either mountain area or coastal area. Indonesia, which is located in the tropical weather, has the cumulonimbus (CB) cloud that produces thunderstorm lightning easily. This condition causes the flashover of the insulator, and if the condition is continued, it leads to the failures of insulators in Indonesia [12-13]. Other than that, due to the high precipitation and pollutant, uneven distribution of electric fields along the shed insulators could make an excessive electric field value in one part. Hereafter, the partial discharge phenomenon could occur. Partial discharge occurrence for a long time may degrade the quality of the polymer insulator [14].

The insulators used have been in service for around 30 years. These are the oldest polymeric insulator have been operating in Indonesia. In the first place, the reason why ceramic and glass insulators were replaced with polymeric insulators was because of the explosion in 1982. The volcanic ash had reached a maximum altitude of 20 km [15]. The pins on the ceramic insulator or the glass insulator are heavily corroded due to a broad scope of ash falls and prolonged recovery time of affected regions, so that the replacement of the ceramic insulator is done quite often. Therefore, the use of polymer insulators began to be applied to this area to overcome the existing problem.

After 30 years in service, two polymeric insulators were taken down to be observed in this research. This paper aims to gain knowledge of the degradation mechanism of field-aging polymeric insulators. A better understanding of what happened in the field is essential to improve the quality of future insulators. The changes in surface structure were analyzed in-depth using advanced techniques by a further physicochemical investigation. Several diagnostic methods were conducted, including Spectroscopy and Scanning Electron Microscopy (SEM), Energy-dispersive X-ray Analysis (EDX), Thermo-Gravimetric Analysis (TGA), and Fourier Transform Infrared (FTIR).

2. Samples under Evaluation

A. Insulator Characteristic

Table 1. Insulator Main Characteristic

Characteristic	**Value**
Voltage Rating (V)	70
Number of Sheds	23
Section Length / X (mm)	976
Shed 1 Diameter / D1 (mm)	93
Shed 2 Diameter / D2 (mm)	78
Leakage Distance (mm)	1905
Arcing Distance (mm)	697

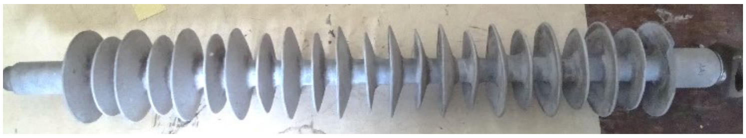

Figure 1. 30 Years-In-Service 70 kV Polymeric Insulator

In this research, four different samples were observed. The insulators used for all four samples have long rod suspension type. The characteristics of the insulator are presented in Table 1. The first and second samples are the natural aging insulators. These two insulators were aged for 30 years under tropical environmental conditions.

Then, two virgin insulators were used to compare with the natural aging insulators. The first virgin sample was the insulator, which never been applied to any treatment. The sample still has a smooth surface and far from deterioration. It is stored in a cool and clean place. The other virgin insulator, virgin-2, is the same as the first sample, which has never been installed in the field. The difference is that the sample was stored under direct sunlight and exposed to rain for two years.

B. Environmental Condition of Aged Insulators

The aged sample was in service since 1989 or operated for 30 years before the insulator was taken for research purposes in 2019. The insulators were installed in the 70 kV transmission. The installed area has a humid tropical climate, which has a significant amount of rainfall during the year; this is true even for the driest month. The average temperature lies between 24°C - 35°C, and high UV radiation occurs during midday hours. About 2589 mm of precipitation falls annually [16-17].

C. Sample Measurements

Physicochemical and electrical analysis techniques evaluated the surface degradation of polymeric insulators. The methods adopted for assessing the field-aging phenomenon were as follows: the wettability of insulator surface, surface morphological degradation assessed by visual inspection and Scanning Electron Microscopy (SEM), a surface material composition by Energy Dispersive X-ray (EDX)and FTIR spectroscopy, thermal stability by thermogravimetric analysis, and last, electrical properties by analyzing the Leakage Current value and the resistance of the polymeric insulators.

The hydrophobicity class of all four samples was investigated by implementing IEC 62073 method A, the contact angle method. This method measures the angle between the edge from a single droplet of water and the horizontal surface. In this research, there is no advancing and receding contact angle. The surface was kept horizontal. The volume of a single water droplet is in the range of 5µl to 50µl. The duration within the application of the droplet and measurement was performed less than a minute. [18]

Scanning electron microscopy (SEM) and X-ray spectroscopy (EDX) is a powerful technique for surface material analysis. This method provides the surface topography at a high resolution focused with excellent depth of field. The primary electron with the energy of 0.5-30 keV enters the surface, and the electron bombards the emission of secondary electrons. The SEM equipped with EDX analysis gives elemental analysis and quantitative compositional information of small-nano areas of the sample. The electron beam from the instrument on the sample surface produces an x-ray that shows the quantitative characteristic of the elements from the material [19]. The instrument used for SEM/EDX analysis was Hitachi SU3500, as seen in figure 2.

Figure 2. Hitachi SU3500 for SEM/EDS Analysis

Before conducting the SEM analysis, the samples used were cleaned with distilled water and cut carefully using a sharp knife with a magnifier's help. The purpose was to maintain the cut surface neat or not heavily textured for the SEM cross-sectional analysis. All the samples had a size of 10 mm x 10 mm approximately. The study was performed using an SEM Hitachi SU3500 equipped with Energy Dispersive X-ray Spectroscopy (EDX) in low vacuum mode at 15 kV acceleration voltage. The silicone rubber samples were sputtered with gold to reduce charging effects. A magnification of 1000x was used to capture the SEM micrographs. The analysis results show differences in the silicone rubber's surface microstructure since the EDX interaction depth of 50 µm.

Fourier transform infrared (FTIR) is the preferred method of infrared spectroscopy. In this analysis, infrared radiation is passed through the sample; some radiation is transmitted and absorbed by the sample. The signal at the detector of FTIR is a spectrum with a specific character that differs one material from others or is called the 'fingerprint' of the sample. The range of the infrared region for FTIR is the mid-infrared region (4000-200 cm^{-1}). A typical FTIR spectrometer consists of a source, interferometer, sample compartment, amplifier, detector, an analog-to-digital converter, and computer. The source gives radiation, which passes through the sample (interferometer) and reaches the sensor. The amplified signal is converted to digital with an A/D converter. Hence, the signal is transferred to the computer, where Fourier transform is gained. There are four major sampling techniques in FTIR; Transmission, Attenuated Total Reflection (ATR), Specular Reflection, and Diffuse

Reflectance [20-21]. In this research, the method used was transmission technique with KBR pellets used.

Figure 3. Shimadzu IRPrestidge-21 for FTIR Analysis

Furthermore, for thermal analysis, the TGA instrument consists of sample pan supported by a precision balance which is resides in furnace for heating purpose. Mass as the main criterion on the analysis is monitored along the experiment period. A sample purge gas, here used nitrogen, controls the sample environment. This gas flows over the sample and out through an exhaust. In this analysis, the TGA instrument quantifies the loss of water and solvent also the decomposition and weight presentation of filler [22]. TGA generally is used to evaluate the thermal stability of the sample. This gives information the onset temperature of material. Over this temperature value the material will start to degrade. Most polymer degrade at the region of 200^{o}C. Polymers are thermally stable where withstand in the temperatures of 300^{o}C in air and 500^{o}C in inert gases without significant structural changes [23].

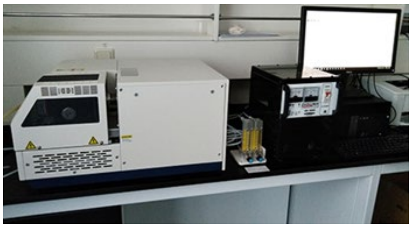

Figure 4. Hitachi STA7300 for TG/DTA Analysis

Thermogravimetric analysis (TGA) is a thermal analysis technique that measures the rate of change and the amount of material weight as a function of temperature or time in a controlled and specific atmosphere. This measurement is primarily used to determine the composition of materials and to predict the thermal stability up to elevated temperatures [24]. Most TGA curves are also equipped with other different curves, DTA and DTG curves. At appropriate temperatures, mass loss is measured and indicated by the first derivative (DTG) of the TGA curve [25]. Thermogravimetric analysis was conducted on virgin and aged samples using Hitachi STA7300. The specimen was cut for the insulator weighing 11.871 mg for the virgin sample and 13.802 mg for the aged sample. Each sample was placed into the center of aluminum analysis pan with tweezers and heated from 30^o C up to 600^o C for two hours. In this study, every sample was analyzed with three different constant heat rates, which were 10^o C/min, 20^o C/min, and 40^o C/min in a nitrogen atmosphere. The nitrogen flow rate itself was 100 ml/min.

Last, for leakage current (LC) experiment, there are two parameters obtained, which are LC magnitude and the waveform. The main aim for the leakage current (LC) measurement is to observed LC waveform characteristics. The two natural aging insulators were set up within rating voltage and Line-to-Line voltage. The output voltage is measured through the voltage divider resistance and observed within the oscilloscope. Based on the value of output voltage, along with its frequency components, the leakage current value can be obtained [26]. The experimental circuit setup for leakage current measurement is shown on figure 5.

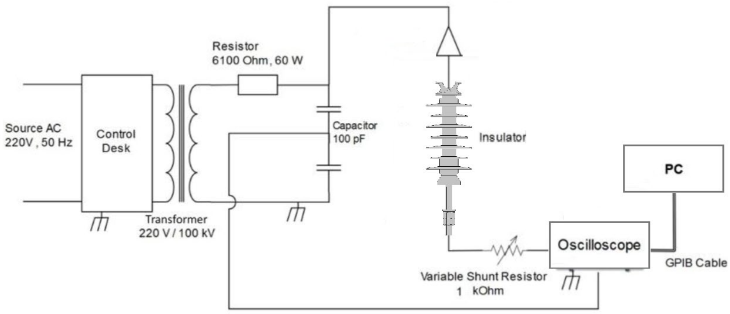

Figure 5. Experimental circuit setup for leakage current measurement

3. Results and Analysis

A. Visual Inspection

As shown on figure 6, surface deterioration of the aged polymeric insulators was visible seen without any help from advanced tools. The most significant changes that were observed are as follows:

- White powder on surface and discoloration
- Contamination or dirt
- Silicone grease on one side
- Fungus contamination on the bottom side
- Sheath cracked and moisture penetration at some sheath points

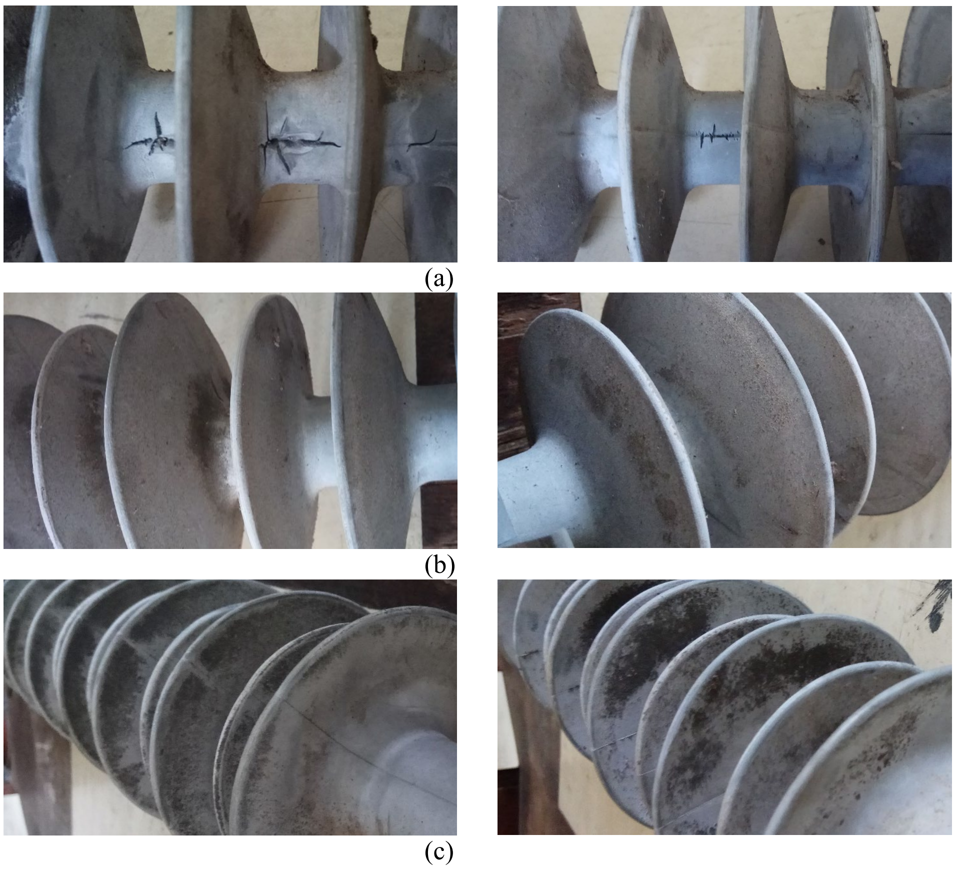

Figure 6. (a) Crack on Aged Insulator Sheath; (b) Upper View of Aged Insulator; (c) Bottom View of Aged Insulator (Left: Natural Aging-1 Sample, Right: Natural Aging-2 Sample)

The cracks were clearly seen on insulator sheath as illustrated on figure 6 (a). For the natural aging-1, it was observed that there were two crack points on the sheath. From left to right crack, that had 30 mm and 38 mm in length. While, for the natural aging-2, there was only one visible crack on the sheath with the length of 28 mm. This severe crack condition was probably due to continual activity of dry discharge and weathering of the material, then if no replacement conducted, exposure of rod is likely to occur [27]. White powder or chalking and discoloration were visible on the upper side of the shed, figure 6 (b). This discoloration phenomenon happened because of the exposure of filler compound due to normal weathering [27]. The high precipitation in the area accelerated oxidative degradation, which leads to the intramolecular cyclization process [28]. On the other side, even though discoloration was minimally seen, the fungus contamination was observed. Also, as seen on figure 6 (c), the silicone grease on polymer insulator sheds on the bottom side existed and slightly more than the sheath and top surfaces. There were spotted crack on sheath parts likely near the energized end, but not on all over the insulator sheath. On both naturally aged insulators, no rod or core was exposed.

B. Hydrophobicity Classification

Table 2. Insulator Main Characteristic

No	Sample	Middle Shed	Top Shed	Cracked Shed
1	Virgin-1			
2	Virgin-2	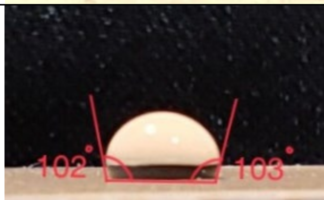		
3	Natural Aging-1	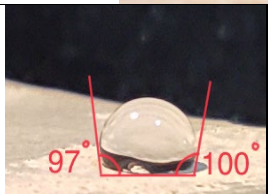	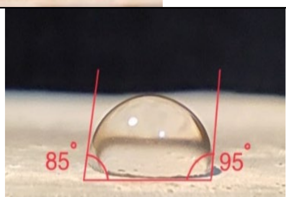	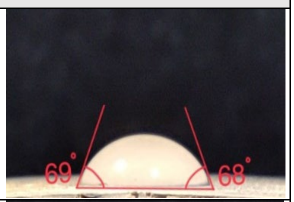
4	Natural Aging-2	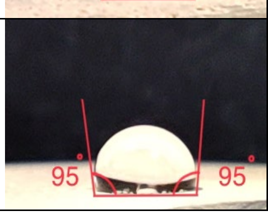	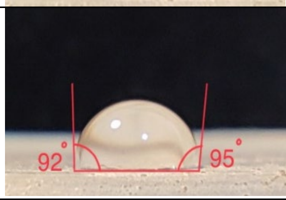	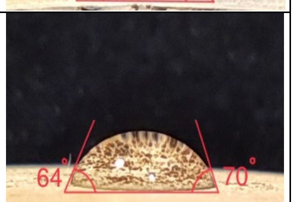

The first component, which is sometimes thought to be the primary thing to consider, is the hydrophobicity of the composite insulator. Before the installation and after being used, observation is highly needed to improve the durability of the insulator. The hydrophobicity of the insulator was assessed using IEC62073, guidance on the measurement of hydrophobicity of the insulator surface [18]. The method used was a single drop from a pipette and taken by a macro lens. There are seven hydrophobicity classification classes (HC), evaluated from most hydrophobic surface (HC1) to least hydrophobic surface (HC7, most hydrophilic surface). The measurement of the contact angle involves the evaluation angle formed between the surface of the insulator and the edge of a single water droplet. In this test, the application of the droplet was done on a horizontal surface. So, there was no receding contact angle observed than the advancing contact angle.

As seen in Table 2, all samples were categorized as hydrophobic class 1 due to the angle value of more than 60°. The virgin-1 sample had an angle of 117° and 119° for each side. Having slightly fewer degrees than the virgin-1, virgin-2, which has been stored for five years, also had an angle of 102°-103°. Whether sample 3-4 had been aged in field for 30 years, those still maintained hydrophobic surface with the angle value around 85°-100° and 64°-70° for the cracked surfaces. Compared with the 17-year insulator, which had a 115° contact angle [14], the angle of the aged sample used in this study only differs slightly—the decreased value of cracked surfaces mainly related to the pollutant contaminant and aging by-products. However, the excellent hydrophobic properties of this silicone rubber material are from a hydrophobicity transfer mechanism correlated with the components of low molecular weight [29-30].

C. SEM Analysis

All samples were captured in a magnification of 1000x with the accelerating voltages of 15 kV where subsurface beam scattering limits the spatial resolution of 50µm. Table 3 shows the figures of virgin-1 and virgin-2 samples. The virgin-1 was a new insulator which had been stored in clean and contamination-free storage. As shown on virgin-1 micrograph, the surface was still in a smooth and homogeneous condition. Meanwhile, the virgin-2 sample had a visible textured surface, and from the cross-sectional view, there was noticeable a shallow crack. But, the visible textured surface was only seen on the direct sun-facing side. Before used for research purpose, the sample was stored under direct sunlight and exposed to rain for two years.

The natural aging SEM micrographs were shown in table 4 for both surface and cross-sectional views. Three different parts of the insulator were taken: middle shed, top shed, and cracked sheath. From natural aging-1, it was noticeable that there was a difference on the surface between the top and middle samples. The top sample had a rougher texture, and from the side view, the deterioration was visible seen more severe. It illustrates the nonlinear effects of various stress along the insulators. Otherwise, for natural aging-2, both shed almost had the same surface boundaries, which did not have a significant difference. From the side view, it was clearly seen that the surfaces were immensely uneven. Quantification for the cracked-sheath depth was obtained from the cross-sectional area (side view). For both samples, the cracked sheaths were seen having the loose and the porosity dispersion of filler material and a deep crack [11].

Table 3. SEM Micropgraphs for Virgin Samples

Virgin-1	Virgin-2	Virgin-2 (Side View)
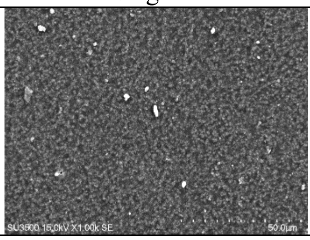	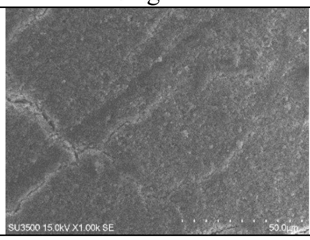	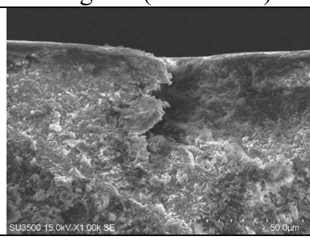

The contamination, including pollutant accumulation and aging residuals during aging process, was concentrated close to the energized side or the top of insulators. The discoloration of shed surfaces was visible mostly on the sun-facing side. This is because solar UV radiation triggered the photo-oxidation of the surface, as reported in [31-32]. Also, the different condition of top and middle shed was possibly occurred due to the electric field strength difference along the insulator. So, the top surface had more severe degradation than the one below. This condition was the same as the previous studies [33-34].

Table 4. SEM Micropgraphs for Natural Aging Samples

No	Sample	Middle Shed	Top Shed	Cracked Shed
1	Natural Aging-1 (Surface View)	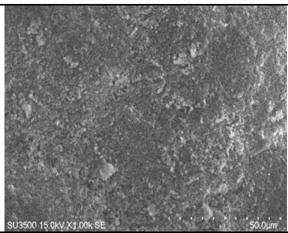	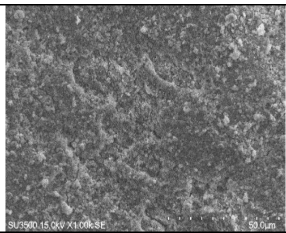	
2	Natural Aging-1 (Cross-sectional View)	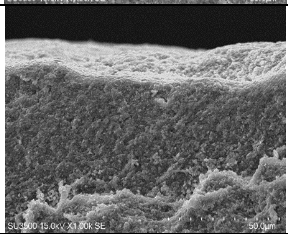	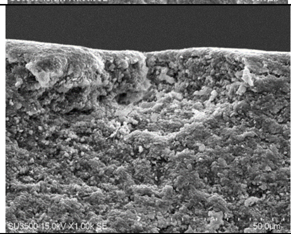	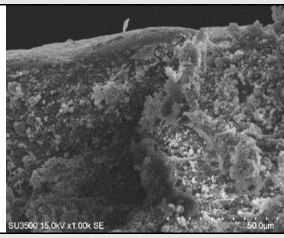
3	Natural Aging-2 (Surface View)	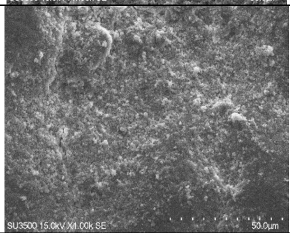	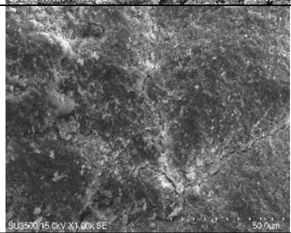	
4	Natural Aging-2 (Cross-sectional View)	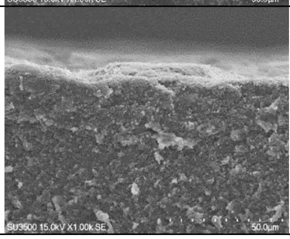	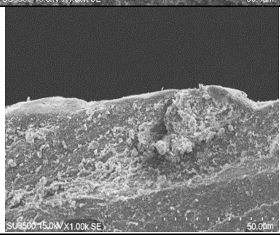	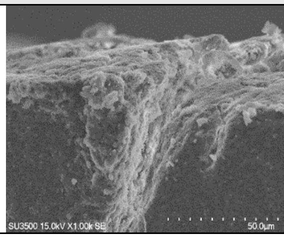

When the virgin sample and the aged samples were compared, as seen on the SEM micrograph, both color and texture were highly different. Even between the aged sample with and without cracked, the more visible difference of texture was found. This happened since the silicone rubber had become more crystalline [8]. In a virgin polymer, the silicone rubber is amorphous, which means a structure with the degree of crystallinity is low. Along the aging process, a restructuration occurred where the crystallinity rises. As the polymer molecules are confined to a definite location, the interaction between filler and polymer is reduced. This is the reason for a crack or even a tracking occurrence [35].

D. EDX Analysis

The EDX analysis had been performed for the virgin and natural aging samples. The results for natural aging-1 and natural aging-2 samples compared with virgin samples are presented in figure 7. The EDX graphs illustrate the peaks for carbon, oxygen, aluminum, and silicone.

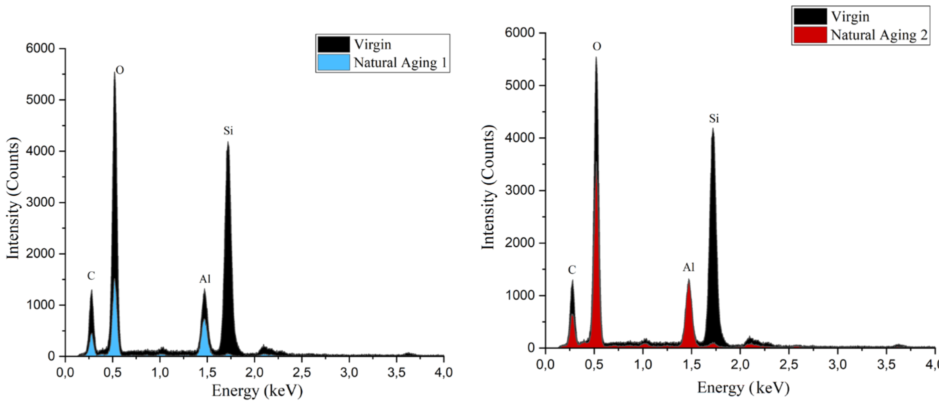

Figure 7. EDX result for virgin sample vs. natural aging sample

The element-composition comparison between aged and virgin material was analyzed using EDX results, as shown in Table 5. The carbon and silicone components were decreased compared with the virgin sample

Table 5. EDX Analysis of the Surface Material (Atomic Percentages of the Heavy Atoms) of the Insulator Housing

Sample	C	O	Al	Si
Virgin	39.22%	47.91%	3.3%	11.57%
Natural Aging 1	38.92% ↓(4.57%)	51.34% ↑(7.15%)	8.81% ↑(166%)	0.29% ↓(97.5%)
Natural Aging 2	33.12% ↓(11.1%)	57.4% ↑(19.8%)	8.34% ↑(152%)	0.41% ↓(96.5%)

(%): changes in elemental composition to virgin material

In contrast, oxygen and aluminum show an increased value. The ratio of aluminum to silicone, a vital parameter in EDX studies, is increased significantly. The silicone value decreased was caused by the thermal decomposition of the silicone rubber matrix and from the ATH filler of insulators. This condition showed a depolymerization occurrence. As seen in table 5, the virgin sample has 11.57 presentation of silicone component, and after aged for 30 years, the value decreased to 0.29% and 0.41% for natural aging-1 and natural aging-2 sample, respectively. This decreased condition agrees with the result of the FTIR analysis. The silicone chain breakdown indicates the fall of this silicone composition because of the photo-oxidation of UV radiation and the thermal effect of aging for a certain period. [37,46]. This condition showed a depolymerization occurrence. In silicone rubber, the silicone-oxygen bond could be broken due to the aging factor. The C/O ratio in the material composition was significantly decreased from 0.82% to 0.76% for Natural Aging-1and 0.58% for Natural Aging-2. The increase of oxygen and decrease of carbon contents were proof of more extensive oxidation of surface material. The higher content of Al, which originated from ATH filler ($Al(OH)_3$), indicated the chalking on the surface material of the insulators, the increased filler concentration on its surface is related to the degradation of the main polymer component.

E. Insulation Resistance and Leakage Current

The resistance test of natural aging insulators was using Megger, and the result value is shown in table 1. The resistance value of Natural Aging-1 was higher than Natural Aging-2. These results agreed with the outcome of SEM, where surface degradation of Natural Aging-1 was less severe than Natural Aging-2. The resistance values within this range allow these polymer insulators to have magnitudes of leakage currents from several to tens μA. In this measurement, the leakage current of each insulator is measured by a change or increase in the source voltage starting from the phase-to-neutral voltage value to the phase-to-phase voltage value of the insulator, so the testing voltage used was at 40 kV to 70 kV. The aim was to see the range of leakage current values of each polymer insulator at its operating voltage.

Table 6. Resistance Test Result for Natural Aging-1 and 2 Samples

No.	Sample	Resistance Value (GΩ)
1	Natural Aging-1	60
2	Natural Aging-2	49

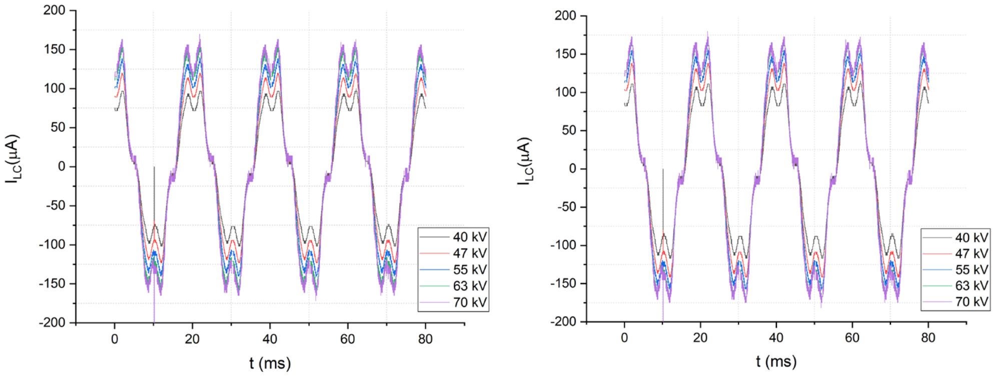

Figure 8. (a) The LC Waveform of Natural Aging-1 and (b) The LC Waveform of Natural Aging-2 Samples at Five Different Voltage Levels

The results of this leakage current measurement were shown in the waveform graph in figure 8, with the comparison chart of the leakage current magnitude in figure 9. Figure 8(a) for Natural Aging-1 sample and compared with figure 8(b) Natural Aging-2 sample, the NA-1 sample had a greater insulator resistance value than the NA-2 sample, which had a lower leakage current. Based on this graph, it could be seen that the 70 kV polymer insulator, which has been operating for 30 years in the field, had a leakage current range between 60-115 μA. Due to this aging factor, it reduced the insulator's performance to withstand stress so that the leakage current increases.

From figure 9, it can be concluded the NA1 had a smaller LC magnitude value compared with NA-2. Especially with the condition of the polymer insulator that had cracked, the tear in the housing had a lower resistance, so that the leakage current increased. This is due to the contribution of the insulator capacitance itself, non-linear resistance, and capacitance of pollutants, which can increase the magnitude of the leakage current flowing on the surface of the polymer insulator. The pollutant that traps water forms a conductive layer, so that larger LC flow occurred on the insulator surface. As a consequence of water molecules trapped on the insulator surface, the increase in the magnitude of LC may be caused by the increase in the conductivity of the insulator surface. If this continuously happens, continuous dry band is started forming which cause to discharge [26, 38].

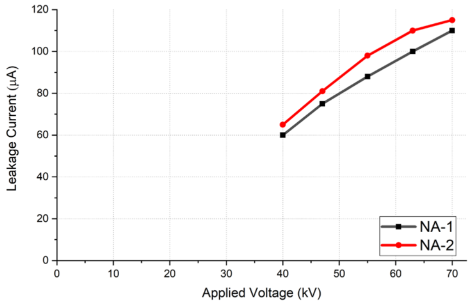

Figure 9. Dependence of Leakage Current on Applied Voltage

F. Thermogravimetric Analysis

Thermogravimetric analysis was conducted to observe the effect of aging on the thermal stability and the thermal degradation behavior [37]. Figure 10 illustrates the results obtained from the TG/DTA measurement of virgin-1 sample at rate of 10 ºC/min. The other three samples has the same typical thermogravimetric graph with virgin-1 sample. The TG plot has multistage decomposition. At the first inclination, the weight loss comprises volatile components such as water and low-molecular-weight solvents. Then, for the second inclination or decomposition step, here occurs loss of massive weight of the main element; in polymeric insulator case, it is the filler. The percentage of mass change of first and second decomposition for virgin-1 sample were 22.4% and 34.14% respectively. From this plot, the onset and endpoint could also be gained. The onset point is a starting point where significant change occurs. Meanwhile, the inflection point is the peak maximum of the decomposition [39]. The onset points of first and second decomposition for virgin-1 samples were 296.3ºC and 424ºC, respectively.

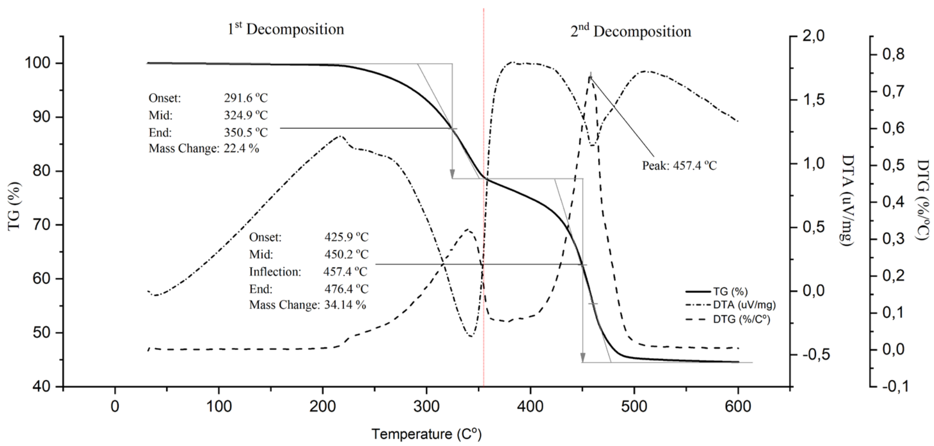

Figure 10. Thermogravimetric Graph for Virgin-1 Sample for 10ºC/min Heat Rate

In this thermogravimetric analysis, the experiments were done at three different heating rates of 10ºC/min, 20ºC/min, and 40ºC/min. The results are seen in figure 10. The decomposition curves of DTG shift toward the higher temperature region with the increase of the heating rate. This is due to the reaction of temperature. The correlation is the higher reaction temperature, the higher reaction rate, hence the lower the oxygen's partial pressure at the gas-solid reaction interface and makes a new equilibrium of reaction. So that the rise in heating rate, the maximum weight loss rate is also increasing.

Table 7. Component value of TG/DTA Graph for Both Inclination

		First Inclination				Second Inclination				
No.	Sample	Onset (°C)	Mid (°C)	End (°C)	Mass Change (%)	Onset (°C)	Mid (°C)	Peak (°C)	End (°C)	Mass Change (%)
Heat Rate 10° C/min										
1	Virgin-1	296.3	327.2	351.0	15.7	424.1	459.2	466.2	507.4	33.40
2	Virgin-2	281.8	316.3	338.3	22.1	422.7	447.7	455.3	470.5	31.80
3	NA-1	281.4	314.9	348.2	21.9	422.5	449.3	457.3	473.4	33.30
4	NA-2	291.6	324.9	350.5	22.4	422.5	450.2	457.4	476.4	34.14
Heat Rate 20° C/min										
1	Virgin-1	306.7	334.8	359.0	16.2	440.7	482.7	491.2	529.9	34.80
2	Virgin-2	293.2	332.3	347.4	22.6	436.0	462.0	466.8	479.4	32.10
3	NA-1	291.0	329.9	355.6	22.0	437.4	460.1	466.1	482.9	33.40
4	NA-2	286.6	328.4	356.1	22.6	433.9	460.9	466.5	484.7	34.26
Heat Rate 40° C/min										
1	Virgin-1	314.5	337.4	360.6	16.5	465.9	508.7	514.8	556.4	35.30
2	Virgin-2	310.1	341.0	363.4	23.1	449.3	473.7	477.4	492.1	33.30
3	NA-1	303.4	339.5	367.8	21.0	448.7	471.7	478.1	482.9	34.40
4	NA-2	313.6	347.6	372.8	28.6	444.2	472.2	480.4	502.4	41.40

The interpretation of DTA and DTG was made simultaneously with the TG plot. The endothermic graph of DTA and the peak point of DTG for both inclinations give the information at which temperature the material is degraded significantly [37]. If only has the TG curve, there is no exact temperature value for the inflection point would be gained. The comparative results for all samples at three different heat rates are tabulated in Table 7. For both decomposition stages, the onset value of the virgin-1 sample for all heat rates was higher compared with three other samples. This is because the virgin-1 sample still has not used or being aged for a certain period. The onset, mid, and end temperature values will increase along with the gain of the heat rate value. The mass change at first inclination of the virgin-1 sample compared with other samples was much lower with an amount ranging from 15.7% to 16.5%, and other samples had 21.0% to 28.6% of mass change.

In contrast, for the second inclination, the mass change value between the virgin sample and the aged sample did not differ significantly and had much alike value. The occurrence of weight loss implies the deterioration of ATH filler of silicone rubber [40]. Based on the first and second decomposition stages, ATH ($Al(OH)_3$) is decomposed in aluminum (Al_2O_3) and water (H_2O) as final products [37]. This slightly different value occurrence shows that the filler of natural-aged-sample material still has a strong bond with its polymer composition. For the natural aged-2 sample, which had a slightly higher value of mass change, 41.4% compared with 31.8-35.3%, was in correspond with the results from SEM/EDX and LC analysis.

G. *FTIR Analysis*

FTIR techniques can be applied to analyze the characterization of silicone rubber. The transmittance values are used for the characterization of the polymer and the filler. Figure 11 shows the FTIR spectra comparisons of the four samples at wavenumbers ranging from 500 to 4000 cm^{-1}. The wavenumbers with significant bands and the corresponding functional groups are shown in Table 8. The concentration of the related bonds is proportional to the peak value of the FTIR transmittance bands. The reduced value of the peak heights of the chemical functional groups of virgin 2 sample and aged samples was caused by the weathering and aging factor [43-44]. From the figure 11, it could be observed that for all aged samples, the peaks of $Si(CH_3)_2$ and $Si\text{-}CH_3$ were decreased, which meant that the side chain was cut and the hydrophobic methyl group was fallen. Hence, this was the cause of the hydrophobic contact angle for the aged sample was reduced. Furthermore, in the waveform at 1000~1100 cm^{-1}, the functional group of Si-O-Si also decreased after being aged for 30 years. The fall of this composition indicated that the main chain of silicone rubber was broken, and the condition has been started to worsen deterioration conditions [45].

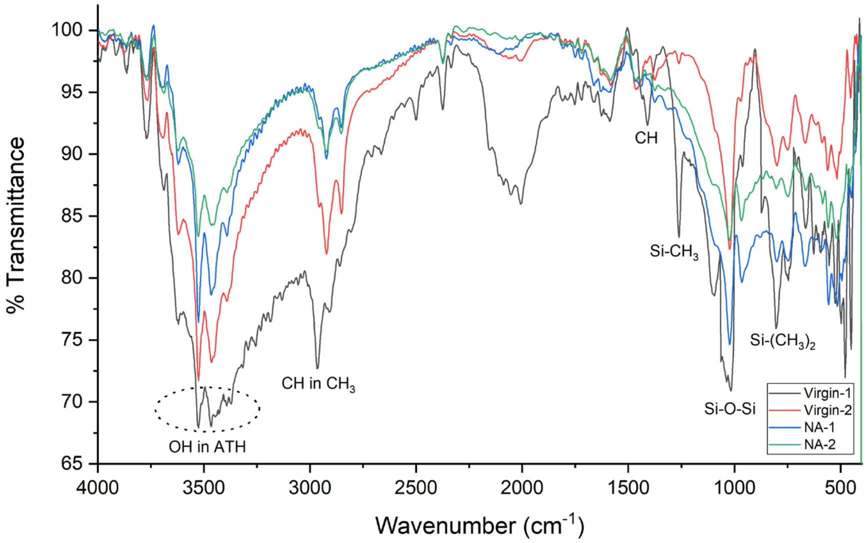

Figure 11. FTIR Transmittance Spectra of Four Different Samples

The reduction of the C-H stretching value for the aged sample was due to the photo-oxidation of UV radiation. So, the impact was the scission of CH_3 bonds and the formation of carbonyl groups; this led to the reduction of surface hydrophobicity level [46]. The bond of O-H in ATH filler for natural aging-1 and natural aging-2 was decreased compared with the virgin sample. The downward peaks regarding these waveform numbers in the transmittance plot illustrated the broken bonds in ATH filler as it aged for an extended period. Moreover, the difference in peak value for natural aging-1 and natural aging-2 was 10% and 20%, respectively. These gave the same results with SEM and TG/DTA, in which the natural aging-2 had more severe conditions than the natural aging-1. This reduction was happened due to the association with the hydroxyl groups, the hydroxyl (OH) stretching of ATH filler [14].

Table 8. FTIR Wavenumber for Each Functional Groups of Silicone Rubber Material [38-39]

Wavenumber (cm^{-1})	Functional Groups	Characteristics
790~840	Si-$(CH_3)_2$	CH_3 stretching vibration
1000~1100	Si-O-Si	SiO stretching vibration
1255~1270	Si-CH_3	CH_3 symmetrical deformation
1412	CH	$CH=CH_2$
2960~2962	CH in CH_3	C-H stretching
3200~3700	OH	OH of ATH, Si-OH

4. Conclusion

The visual observation and physicochemical properties of naturally aged silicone rubber insulator were tested and analyzed in this paper. From several tests conducted, it is found that several performances were degraded to some extent. Based on visual inspection test, the surface of insulators has a moderate degradation. All four samples still had hydrophobic class 1. Chalked and discoloured surface only existed on near end energized sheds, contamination on several bottom side of sheds and crack only in one or two points on insulator sheath. SEM micrograph results for aged insulators show that one of the insulators sample for the top shed and middle shed had a same severe condition and the other sample still in moderate degradation condition. From the EDX result, the C/O ratio in the material composition was decreased from 0.82% to 0.76% for Natural Aging-1and 0.58% for Natural Aging-2.

Furthermore, from TG/DTA analysis, the results of aged samples did not differ greatly compared with the virgin sample. The occurrence of weight loss implies the deterioration of ATH filler of silicone rubber. Based on the first and second decomposition stages, the percentage difference between virgin and aged sample only lower than 4% and lower than 1%. Last, the FTIR spectra shows in general reduction of major chemical composition of the insulator surface, indicating a normal aging condition of the silicone rubber. The difference in peak value for natural aging-1 and natural aging-2 was 10% and 20%, respectively. These results are significant in that the aged silicone rubber insulators suffered just a moderate deterioration despite the fact that insulators had been installed for 30 years and the weather is quite severe. There is high precipitation throughout the year and high UV radiation in midday.

5. References

[1]. Edward A. Cherney, "50 Years in the Development of Polymer Suspension-Type Insulators", *IEEE Electrical Insulation Magazine*, vol. 29, pp. 18–26, 2013.

[2]. F. Weinhold and R. West, “The Nature of the Silicon–Oxygen Bond”, *Organometallics-American Chemical Society,* vol. 30, pp. 5815–5824, 2011.

[3]. J. F. Hall and task force members, "History and bibliography of polymeric insulators for outdoor applications," *IEEE Trans. Power Del.,* vol. 8, pp. 376–385, 1993.

[4]. E. A. Cherney, J. T. Burnham, and R. S. Gorur, Outdoor Insulators. Phoenix, AZ: Ravi S. Gorur Inc., 1999.

[5]. A. S. Maxwell, W. R. Broughton, G. Dean, and G. D. Sims, “Review of Accelerated Ageing Methods and Lifetime Prediction Techniques for Polymeric Materials”, National Physical Laboratory, Teddington, Middlesex, United Kingdom, NPL Rep. DEPC MPR 016, March 2005.

[6]. L. H. Meyer, E. A. Cherney, and S. H. Jayaram, "The role of inorganic fillers in silicone rubber for outdoor insulation: Alumina tri-hydrate or silica," *IEEE Electr. Insul. Mag.*, vol. 20, pp. 13–21, 2004.

[7]. Amin S., Amin. M., "Natural Aging of Sir Insulators in Pakistan," *International Conference on Emerging Technologies*, pp. 114-117, 2009.

[8]. R. Sundararajan, A. Mohammed, N. Chaipanit, "In-service Aging and Degradation of 345 kV EPDM Transmission Line Insulators in a Coastal Environment", *IEEE Trans. Dielectr. Electr. Insul.*, vol. 11, pp. 348–361, 2004.

[9]. M. A. R. M. Fernando, S. M. Gubanski, "Ageing of Silicone Rubber Insulators in Coastal and Inland Tropical Environment," *IEEE Trans. Dielectr. Electr. Insul.*, vol. 17, pp. 326–333, 2010.

[10]. S. M. Rowland, Robertson, Y. Xiong, "Electrical and Material Characterization of Field-aged 400 kV Silicone Rubber Composite Insulators," *IEEE Trans. Dielectr. Electr. Insul.*, vol. 17, pp. 375–383, 2010.

[11]. N. C. Mavrikakis, P. N. Mikropoulos, "Evaluation of Field-ageing Effects on Insulating Materials of Composite Suspension Insulators," *IEEE Trans. Dielectrics and Insulations.,* vol. 2, pp. 490–498, 2017.

[12]. R. Zoro, “Tropical Lightning Current Parameters and Protection of Transmission Lines,” *International Journal of Electrical Engineering and Informatics*, vol. 11, pp. 506-514, September 2019.

[13]. A. S. Ghoniem, “Effective Elimination Factors to the Generated Lightning Flashover in High Voltage Transmission Network,” *International Journal of Electrical Engineering and Informatics*, vol. 9, pp. 455-468, September 2017.

[14]. Suwarno, “Partial Discharge in High Voltage Insulating Materials,” *International Journal of Electrical Engineering and Informatics*, vol. 8, pp. 147-163, March 2016.
[15]. A. Gourgaud, G. Camus, M. C. Gerbe, J. M. Morel, A. Sudradjat, and P. M. Vincent, "The 1982–83 Eruption of Galunggung (Indonesia): A Case Study of Volcanic Hazards with Particular Relevance to Air Navigation", In Latter J.H. (eds) Volcanic Hazards IAVCEI Proceedings in Volcanology vol 1, Berlin: Springer, 1989.
[16]. [Online]. Available: https://www.gismeteo.com/weather-garut-10804/tomorrow/#uvb.
[17]. [Online]. Available: https://www.garutkab.go.id/page/klimatologi.
[18]. *Guidance on the Measurement of Hydrophobicity of Insulator Surface*, IEC 62073, 2016.
[19]. J. I. Goldstein, and D. E. Newbury, “Scanning Electron Microscopy and X-Ray Microanalysis," New York, USA: Springer, 2018.
[20]. W. D. Perkins, "Fourier Transform-Infrared Spectroscopy", Part 1 Instrumentation Topics in Chemical Instrumentation Journal of Chemical Education, January 1986.
[21]. D. A. Skoog, and J. J. Leary, "Principles of Instrumental Analysis, 4th Ed.", Philadelphia: Harcourt Brace Jovanovich., 1992.
[22]. T. Hatakeyama, and F.X. Quinn, "Thermal Analysis: Fundamentals and Applications to Polymer Science Second Edition," West Sussex, England: John Wiley & Sons, Inc., 1999.
[23]. X. Liu, and W. Yu, "Evaluating the Thermal Stability of High Performance Fibers by TGA,” *Journal of Applied Polymer Science*, vol. 99, pp. 937–944, 2006
[24]. S. Sauerbrunn, and P. Gill, "Decomposition Kinetics Using Thermogravimetric Analysis," TA Instruments.
[25]. B. Bacher, M. Walker, and A. Riga, “Thermal Analysis Unlocks the Secrets of Elastomers, Cleveland,” Ohio: NSL Analytical, 2013.
[26]. Rachmawati, N. Sartika, N. R. M. Putra, and Suwarno, "The Study on Leakage Current Characteristics and Electrical Properties of Uncoated Ceramic, RTV Silicon Rubber Coated Ceramic, and Semiconducting Glazed Outdoor Insulators,” *International Journal of Electrical Engineering and Informatics*, vol. 10., pp. 318-336, June 2018.
[27]. "*Field Guide for Visual Inspection of Polymer Insulators*," EPRI, 2015.
[28]. N. Grassie and G. Scott, “Polymer Degradation and Stabilization,” New York, USA: Cambridge University Press, 1985.
[29]. J. Kindersberger and M. Kuhl, "Effect of hydrophobicity on insulator performance," 6th *Int’l. Sympos. High Voltage Eng.*, vol.01, pp. 1-4, 1989.
[30]. H. Hillborg and U. W. Gedde, "Hydrophobicity changes in silicone rubbers," *IEEE Trans. Dielectr. Electr. Insul.*, vol. 6, pp. 703-717, 1999.
[31]. S.M. Rowland, Y. Xiong, J. Robertson, and S. Hoffmann, "Aging of silicone rubber composite insulators on 400 kV transmission lines", *IEEE Trans. Dielectr. Electr. Insul.*, Vol. 14, pp. 130-136, 2007.
[32]. Y. Xiong, S. M. Rowland, J. Robertson, and R. J. Day, "Surface analysis of asymmetrically aged 400 kV silicone rubber composite insulators", *IEEE Trans. Dielectr. Electr. Insul.*, vol. 15, pp. 763-770, 2008.
[33]. A. E. Vlastos and S. M. Gubansi, "Surface Structural Changes of Naturally Aged Silicone and EPDM Composite Insulator," *IEEE Trans. Power Del.*, vol. 6, pp. 888-900, 1991.
[34]. A. E. Vlastos and E. Sherif, "Natural Aging of EPDM Composite Insulators," *IEEE Trans. Power Del.,* vol. 5, pp. 406-414, 1990.
[35]. R. S. Gorur, E. A. Cherney, R. Hackam, and T. Orbeck, "The Electrical Performance of Polymeric Insulating Materials Under Accelerated Aging in a Fog Chamber," *IEEE Trans. Power Del.*, pp. l157-1163, 1988.
[36]. R. S. Gorur, G. G. Karady, A. Jagota, M. Shah, and A. M. Yates, "Aging in Silicone Rubber used for Outdoor Insulation," *IEEE Trans. Power Del.*, vol. 7, pp. 525-532, 1992.

[37]. A. Schindler, M. Doedt, S. Gezgin, J. Menzel, and S. Schmolze, "Identification of polymers by means of DSC, TG, STA and computer-assisted database search," *Journal Thermal Analysis Calorim*, Springer, 2017.

[38]. Suwarno, "Study on the Wave Form of Leakage Current on the 20 kV Post-Pin Ceramic Insulators Under Various Conditions," *Int. Symp. on Electrical Insulating Materials*, pp. 387-390, 2001.

[39]. Su Wei-Fang, "Principles of Polymer Design and Synthesis," Germany, Berlin: Springer, 2013.

[40]. N. Yoshimura, and S. Kumagai, "Electrical and environmental aging of silicone rubber used in outdoor insulation," *IEEE Trans. Dielectr. Electr. Insul.* vol. 6, pp. 632–650, 1999.

[41]. K. O. Papailiou, and F. Schmuck, "Silicone Composite Insulators Materials, Design, Applications," Berlin: Springer-Verlag, 2013.

[42]. "*Fingerprinting of polymeric insulating materials for outdoor use*," CIGRE WG D1.27 TB No. 595, 2014.

[43]. I. F. Husein, C. Chan, S. Qin, and P.K. Chu, "The Effect of High-dose Nitrogen Plasma Immersion Ion Implantation on Silicone Surfaces", *Journal Phys. D: Appl. Physics.,* vol. 33, pp. 2869-2874, 2000.

[44]. N. Chaipanit, R. Chaiwat, and R. Sundararajan, "Accelerated Multistress Aging of Polymeric Insulators under San Francisco Coastal Environment", *IEEE CEIDP*, pp. 636-639, 2001.

[45]. Z. Zhijin, L. Tian, J. Xingliang, L. Chen, Y. Shenhuan, and Z. Yi, "Characterization of Silicone Rubber Degradation Under Salt-Fog Environment with AC Test Voltage," *IEEE Access,* vol. 7, 2019.

[46]. C. Rattanakhogviput, A. Mohammed, C. Ayerh, E. Soundarajan, and R. Sundararajan, "Surface Analysis of Polymeric Surge Arresters under Coastal Florida Conditions," *Annual Report Conference on Electrical Insulation and Dielectric Phenomena*, 2002.

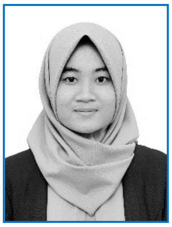

Lunnetta Safura Lumba was born in Indonesia in 1996. She completed the B.Sc. and M.Sc. degree in Electrical Power Engineering at Institut Teknologi Bandung, Indonesia in 2017 and 2018 respectively. She had worked for some years on power system consultant group. She is currently a research assistant in Electrical Power Engineering Research Group, Institut Teknologi Bandung.

Suwarno was born in Indonesia in 1965. He received B.Sc. and M.Sc. from The Department of Electrical Engineering, Institut Teknologi Bandung, Bandung, Indonesia in 1988 and 1991 respectively. He received PhD from Nagoya University, Japan in 1996 in the field of High Voltage Electrical Insulation. Prof. Dr. Suwarno is a professor in The School of Electrical Engineering and Informatics, Institut Teknologi Bandung and currently he is the Chairman of Electrical Power Engineering Research Group and a senior member of IEEE.